

Mushroom Tyrosinase: Catalase Activity, Inhibition, and Suicide Inactivation

FRANCISCO GARCÍA-MOLINA,[†] ALEXANDER N. P. HINER,[†] LORENA G. FENOLL,[†]
 JOSÉ N. RODRÍGUEZ-LOPEZ,[†] PEDRO A. GARCÍA-RUIZ,[‡]
 FRANCISCO GARCÍA-CÁNOVAS,^{*,†} AND JOSÉ TUDELA[†]

GENZ: Grupo de Investigación de Enzimología, Departamento de Bioquímica y Biología
 Molecular-A, Facultad de Biología, and Departamento de Química Orgánica, Facultad de Química,
 Universidad de Murcia, E-0100 Espinardo, Murcia, Spain

Mushroom tyrosinase exhibits catalase activity with hydrogen peroxide (H₂O₂) as substrate. In the absence of a one-electron donor substrate, H₂O₂ is able to act as both oxidizing and reducing substrate. The kinetic parameters V_{\max} and K_m that characterize the reaction were determined from the initial rates of oxygen gas production ($V_0^{O_2}$) under anaerobic conditions. The reaction can start from either of the two enzyme species present under anaerobic conditions: *met*-tyrosinase (E_m) and *deoxy*-tyrosinase (E_d). Thus, a molecule of H₂O₂ can reduce E_m to E_d via the formation of *oxy*-tyrosinase (E_{ox}) ($E_m + H_2O_2 \rightleftharpoons E_{ox}$), E_{ox} releases oxygen into the medium and is transformed into E_d , which upon binding another molecule of H₂O₂ is oxidized to E_m . The effect of pH and the action of inhibitors have also been studied. Catalase activity is favored by increased pH, with an optimum at pH = 6.4. Inhibitors that are analogues of *o*-diphenol, binding to the active site coppers diaxially, do not inhibit catalase activity but do reduce diphenolase activity. However, chloride, which binds in the equatorial orientation to the protonated enzyme (E_mH), inhibits both catalase and diphenolase activities. Suicide inactivation of the enzyme by H₂O₂ has been demonstrated. A kinetic mechanism that is supported by the experimental results is presented and discussed.

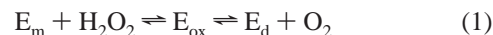
KEYWORDS: Tyrosinase; mushroom; catalase; inhibition; suicide inactivation

INTRODUCTION

Tyrosinase (EC 1.14.18.1), often also referred to as polyphenol oxidase (PPO), is a copper-containing mono-oxygenase, present in a diverse range of organisms, that is responsible for melanization in animals and the enzymatic browning of fruit. The enzyme catalyzes two distinct reactions involving molecular oxygen: the hydroxylation of monophenols to *o*-diphenols and the oxidation of the latter to *o*-quinones (1–3).

Chemical and spectroscopic studies of tyrosinase have shown that its binuclear copper active site can be prepared in several forms: *met*, *deoxy*, and *oxy* (4–6). The oxygenated form, *oxy*-tyrosinase (E_{ox}), is capable of acting on both monophenols and *o*-diphenols. *met*-tyrosinase (E_m) does not act on monophenols but can be converted to E_{ox} by the addition of hydrogen peroxide (H₂O₂) (4–6). *deoxy*-Tyrosinase (E_d) will bind molecular oxygen (O₂) to form E_{ox} (6). Most of the enzyme in a freshly prepared sample (resting tyrosinase) is in the E_m form unable to bind O₂; only a small fraction is present as E_{ox} , this being necessary to initiate catalysis with monophenols (7).

Recently, a mechanism has been published for the catalase activity of a catechol oxidase (CAO) isoenzyme from *Ipomoea batatas* (sweet potato) (8). These ubiquitous plant enzymes lack monooxygenase activity in contrast to tyrosinase (9). CAO and tyrosinase, together with hemocyanin, the O₂ transport protein of many arthropods, possess an antiferromagnetically coupled dinuclear copper center in the *met* and *oxy* states. These so-called type-3 copper centers bind and/or activate O₂ (10, 11) and share similar spectroscopic features (12). Catalase activity has been described in several hemocyanins (13–15). In this case, the proposed mechanism is initiated by the binding of the first H₂O₂ molecule to the reduced (Cu⁺Cu⁺) *deoxy* state of the copper oxidizing it to Cu²⁺Cu²⁺ (*met*-hemocyanin). The second H₂O₂ now enters the active site and forms the *oxy* state with the dinuclear copper. The H₂O₂ is then oxidized to O₂, and the copper returns to the Cu⁺Cu⁺ state. The catalase cycle has not been described in the case of tyrosinase, although the following reaction was described some time ago (4–6).



In the case of CAO, catalase activity has been described in one isoenzyme (8). The proposed mechanism involves binding of the first H₂O₂ to the *met* form, displacing a hydroxo group bound

* Author to whom correspondence should be addressed [fax +34 968 363963; e-mail canovasf@um.es].

[†] Facultad de Biología.

[‡] Facultad de Química.

to the coppers, to form the *oxy* state with the peroxide bound in the tetragonal planar $\mu\text{-}\eta^2\text{:}\eta^2$ mode. The carboxyl group of Glu236 is oriented in such a way that it facilitates the monodentate union of a second H_2O_2 to the *oxy* enzyme. This H_2O_2 then deprotonates and rearranges to a *cis*- $\mu\text{-}\eta^1\text{:}\eta^1$ binding mode to the copper centers. Finally, the second peroxide (*cis*- $\mu\text{-}\eta^1\text{:}\eta^1$) is oxidized to O_2 and the first ($\mu\text{-}\eta^2\text{:}\eta^2$) is reduced to water and a hydroxo group, regenerating the *met* form. Note that in this mechanism two molecules of H_2O_2 must bind the *met* form before O_2 release.

Catalase activity has also been described in another group of enzymes, the peroxidases (16). Heme peroxidases have been classified in three classes (17). The classification is based on sequence comparisons and enzyme localization rather than on function. In a series of papers, we studied catalase activity in peroxidases from each of the classes. From class I, recombinant pea cytosolic ascorbate peroxidase was studied and was found to not exhibit catalase activity, but it was inactivated by H_2O_2 (18). In the case of class II, lignin peroxidase (*Phanerochaete chrysosporium*) and *Arthromyces ramosus* peroxidase were examined. Both enzymes exhibited catalase activity with hyperbolic H_2O_2 concentration dependence and also underwent suicide inactivation with H_2O_2 (19). The class III enzymes horseradish peroxidase C (HRP-C) (20, 21), horseradish peroxidase isoenzyme A2 (22), and isoperoxidase-B2 from *Lupinus Albus* hypocotyls (23) all demonstrated catalase activity and suicide inactivation with H_2O_2 .

Others have described catalase activity in chloroperoxidase (24) and bacterial catalase-peroxidase (class I) (25, 26). Additionally, focusing on possible biotechnological applications (e.g., biosensors, bioreactors, or assays), a comparative study of the inactivation by H_2O_2 of commercially available horseradish peroxidase isoenzymes A and C has been performed (27).

Physiological explanations have been sorted to explain catalase activity in noncatalase enzymes. Situations can arise in the apoplast in which there is an imbalance between oxidants and reducing compounds either through an increase in H_2O_2 levels (oxidative burst) and the generation of other hydroperoxides (28–30) or through a fall in the concentrations of reductants (such as ascorbate or phenols (31, 32)). In such situations, peroxidases may suffer an irreversible inactivation process, and catalase activity may partially protect them. Bacterial and fungal infections in plants lead to a burst of H_2O_2 formation. Although, as mentioned above, peroxidases may be inactivated, tyrosinase can use part of this H_2O_2 to generate *o*-quinones that also form part of the defense mechanism against infection (2). Mushroom tyrosinase can also be taken as a model and reference enzyme for tyrosinase activity in tumor cells (melanomas) in which increased levels of tyrosinase induced by H_2O_2 have been described (33).

This paper describes the kinetic characterization of the catalase activity of tyrosinase measured by O_2 production. The actions of different types of inhibitors and suicide inactivation of the enzyme are discussed. A mechanism consistent with the kinetic data is proposed and compared and contrasted to the equivalent process in hemocyanin, CAO, and peroxidase. Possible physiological implications are discussed.

MATERIALS AND METHODS

Reagents. Mushroom tyrosinase (3300 units/mg), bovine erythrocyte superoxide dismutase (SOD) (4200 units/mg), 4-*tert*-butylcatechol (TBC), mannitol, tropolone, and salicylhydroxamic acid were from Sigma/Aldrich (Madrid, Spain). H_2O_2 (30% v/v) (analytical reagent grade) was obtained from Merck. Stock solutions of reducing substrate

were prepared in 0.15 mM phosphoric acid to prevent autoxidation. Milli-Q System (Millipore Corp.) ultrapure water was used throughout this research.

Enzyme Purification. Commercial mushroom tyrosinase was purified by Duckworth and Coleman's procedure (34) but with two additional chromatographic steps (35). Protein concentrations were determined by Bradford's method (36) using bovine serum albumin as standard.

Tyrosinase Activity. The diphenolase activity of tyrosinase was determined spectrophotometrically by measuring 4-*tert*-butyl-*o*-benzoquinone accumulation at 400 nm ($\epsilon = 1150 \text{ M}^{-1} \text{ s}^{-1}$) (37) during 4-*tert*-butylcatechol oxidation, using a Perkin-Elmer Lambda-35 spectrophotometer. Assay conditions are given in the figure legends.

Oxygen Production. Oxygen production was measured with a Clark-type electrode coupled to a Hansatech Oxygraph (King's Lynn, Norfolk, UK). The equipment was calibrated using the tyrosinase 4-*tert*-butylcatechol method (38). Nitrogen was bubbled through the stirred reaction medium to remove oxygen. The reaction medium (2 mL) contained H_2O_2 at different concentrations (see figures) in the following buffers: 45 mM sodium acetate (pH 3.63, 4.05, 4.51, 5.10, 5.40, and 5.76), 45 mM sodium phosphate (pH 6.15, 6.54, 7.00, 7.39, 7.70, and 8.00). The reactions were started by the addition of tyrosinase in water. Two types of experiments were performed with the system described.

Determination of the Initial Rate of H_2O_2 -Decomposing Activity ($V_0^{\text{O}_2}$). Values of $V_0^{\text{O}_2}$ were determined at short reaction times from triplicate measurements at each $[\text{H}_2\text{O}_2]$. From experiments studying the dependence on $[\text{H}_2\text{O}_2]$, $V_{\text{max}}^{\text{O}_2}$ and $K_m^{\text{H}_2\text{O}_2}$ were obtained by nonlinear regression to a plot of $V_0^{\text{O}_2}$ against $[\text{H}_2\text{O}_2]$ by using the program SigmaPlot for Windows (version 2; Jandel Scientific Software, San Rafael, CA) (39).

Determination of the Oxygen Produced at the End of the Reaction ($[\text{O}_2]_{\infty}$). In this case, the end of reaction was reached when no further O_2 production was observed. From these measurements, the stoichiometry of the reaction at limiting $[\text{H}_2\text{O}_2]$ was determined.

Suicide Inactivation of Tyrosinase by H_2O_2 . The inactivation of tyrosinase was performed at 25 °C in 2 mL incubations at pH 7.0 (45 mM sodium phosphate buffer). The experiment was done in both anaerobic (continuous N_2 bubbling) and aerobic conditions. The reaction medium contained 0.6 μM enzyme and 5 mM or 30 mM H_2O_2 . At the times indicated, aliquots were removed and the catalase activity was measured (pH = 7.0, $[\text{H}_2\text{O}_2] = 5 \text{ mM}$). Experiments were performed in triplicate at each $[\text{H}_2\text{O}_2]$.

RESULTS AND DISCUSSION

Oxygen Production. Tyrosinase is able to produce molecular oxygen when it is incubated with H_2O_2 as the sole substrate. The time-course plots for oxygen production are shown in **Figure 1**, allowing calculation of the initial rates of oxygen production ($V_0^{\text{O}_2}$). The $V_0^{\text{O}_2}$ values exhibited a linear dependence on enzyme concentration (**Figure 1A**, inset). In addition, the hyperbolic dependence of $V_0^{\text{O}_2}$ on the H_2O_2 concentration revealed that saturation kinetics were being observed under steady-state conditions; thus, values for $K_m^{\text{H}_2\text{O}_2}$ and $k_{\text{cat}}^{\text{O}_2}$ could be obtained from the data (**Figure 1**, inset). In **Table 1**, the values obtained are shown in comparison to those for hemocyanin, CAO, and various peroxidases (8, 19–26).

The efficiency of tyrosinase ($k_{\text{cat}}^{\text{O}_2}/K_m^{\text{H}_2\text{O}_2} = (5.5 \pm 1.1) \times 10^2 \text{ M}^{-1} \text{ s}^{-1}$) was lower than those of chloroperoxidase (24) and catalase-peroxidase (26).

Addition of Superoxide Dismutase and Mannitol. The O_2 that is made as a result of the catalase activity of HRPC was at one time proposed to originate from the dismutation of $\text{O}_2\text{•}$; we showed that this is a minority route (21). To study if free radicals are implicated in the formation of O_2 from H_2O_2 by tyrosinase, that is, if it is a radical mechanism, superoxide dismutase (SOD) was added to the medium. **Figure 2** shows the data for the formation of O_2 in the presence and absence of SOD, and it is clear that there is no difference in the rates of O_2 generation. A

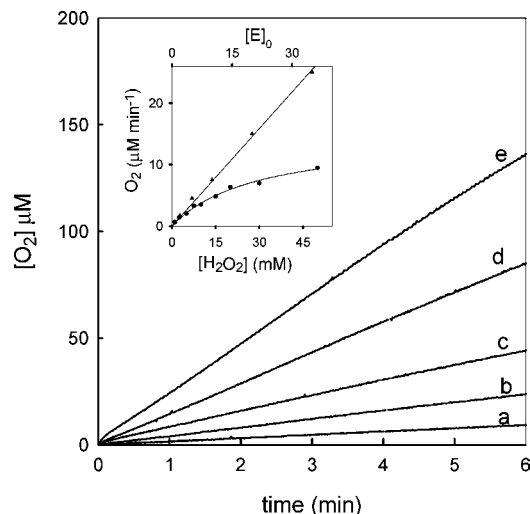


Figure 1. Dependence of oxygen production on time, and H_2O_2 and enzyme concentrations. Time courses of oxygen production in a catalase-like reaction between tyrosinase and H_2O_2 . The reactions were started by the addition of different concentrations of enzyme, as shown to 2 mL reaction medium containing 6 mM H_2O_2 in 45 mM sodium phosphate buffer, pH 7.0 at 25 °C. $[\text{E}]_0$ (a) 10 nM; (b) 25 nM; (c) 50 nM; (d) 100 nM; (e) 175 nM. Inset: Plots of initial rate of oxygen production ($V_0\text{O}_2$) against tyrosinase concentration ($[\text{H}_2\text{O}_2] = 5$ mM) and $V_0\text{O}_2$ against H_2O_2 concentrations ($[\text{E}]_0 = 15$ nM).

Table 1. Kinetic Data of Catalase Activity in Mushroom Tyrosinase, Catechol Oxidase, Hemocyanin, and Peroxidase^a

| | $k_{\text{cat}}\text{O}_2$ (s^{-1}) | $K_{\text{m}}\text{H}_2\text{O}_2$ (mM) | efficiency: $k_{\text{cat}}\text{O}_2/K_{\text{m}}\text{H}_2\text{O}_2$ ($\text{M}^{-1}\text{s}^{-1}$) | ref |
|---------|--|---|---|------------|
| AbTyr | 16.4 ± 1.1 | 29.7 ± 4.2 | $(5.5 \pm 1.1) \times 10^2$ | this paper |
| lbCAO | $(6.3 \pm 1.8) \times 10^{-2}$ | 1.18 ± 0.05 | 53 ± 17 | 8 |
| LpHC | $(11.5 \pm 1.8) \times 10^{-2}$ | 0.50 ± 0.03 | $(2.3 \pm 0.53) \times 10^2$ | 8 |
| McHC | $(20.7 \pm 2.5) \times 10^{-2}$ | 1.20 ± 0.06 | $(1.72 \pm 0.3) \times 10^2$ | 8 |
| HRPC | 1.78 ± 0.12 | 4.0 ± 0.6 | $(4.45 \pm 0.93) \times 10^2$ | 20 |
| HRPC-A2 | 2.2 | 23 | 95 | 22 |
| ARP | 1.15 ± 0.09 | 10.2 ± 2.3 | $(1.12 \pm 0.32) \times 10^2$ | 19 |
| LiP | 2.87 ± 0.21 | 8.6 ± 0.4 | $(3.33 \pm 0.39) \times 10^2$ | 19 |
| CPO | $(9 \pm 1) \times 10^2$ | 3.3 ± 0.4 | $(2.72 \pm 0.62) \times 10^5$ | 24 |
| LalB2 | 6.7 | 5 | 1.34×10^3 | 23 |
| E.C HPI | 16.3×10^3 | 3.9 | 4.17×10^6 | 26 |

^a AbTyr, tyrosinase from *Agaricus bisporus* (mushroom); lbCAO, catechol oxidase from *Ipomea batatas* (sweet potato); LpHC, hemocyanin from *Limulus polyphemus*; McHC, hemocyanin from *Megathura crenulata*; HRPC, horseradish peroxidase isoenzyme C; HRP-A2, horseradish peroxidase isoenzyme A2; ARP, peroxidase from *Arthromyces ramosus*; LiP, lignin peroxidase from *Phanerochaete chrysosporium*; CPO, chloroperoxidase from *Caldariomyces fumago*; LalB2, isoperoxidase B2 from *Lupinus albus* hypocotyls; EchPI, *Escherichia coli* hydroperoxidase I (catalase-peroxidase).

similar effect was obtained after the addition of mannitol to the reaction medium (Figure 2). These data suggest that free radicals are not involved in the mechanism.

Participation of E_d in Turnover of Tyrosinase Catalase Activity. It is known that native tyrosinase is mainly in the E_m form with around 10–30% present as E_{ox} (9). E_d was formed by passing N_2 through the sample to induce anaerobicity and adding catalytic quantities of TBC, which through the reaction $\text{E}_m + \text{D} \rightleftharpoons \text{E}_m\text{D} \rightarrow \text{E}_d + \text{Q}$ produces E_d . In Figure 2, inset, it can be seen that the addition of E_d , made under anaerobic conditions (curve b), initiates enzyme turnover at the same velocity as native enzyme (curve a). From these experiments, it is clear that the three enzymatic forms, E_m , E_d , and E_{ox} , that

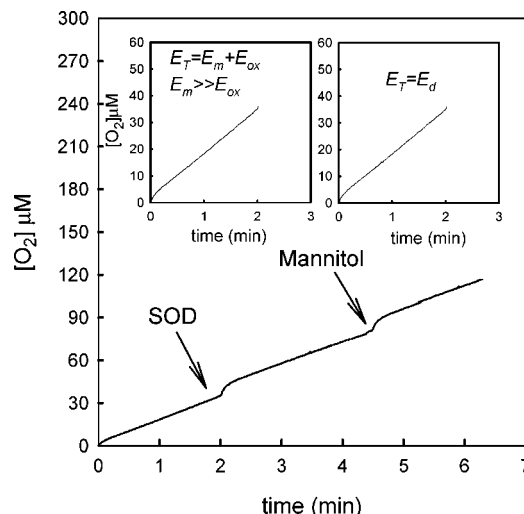


Figure 2. Action of different effectors on the catalase activity of tyrosinase. The reactions were carried out in 45 mM sodium phosphate buffer pH 7.0 at 25 °C. Oxygen formation in an assay containing 0.12 μM tyrosinase and 6 mM H_2O_2 . On addition (arrows) of SOD (0.5 μM) or mannitol (3 mM), no rate changes were observed. Inset: Generation of E_d . (a) Oxygen production in an assay containing 0.12 μM tyrosinase and 6 mM H_2O_2 in 45 mM sodium phosphate buffer, pH 7.0 at 25 °C. (b) In the same conditions, but the enzyme has previously been bubbled with N_2 , and at 5 min a catalytic quantity of TBC was added ($\text{E}_m \rightarrow \text{E}_d$). After 15 min, the enzyme sample (0.12 μM) was added to the oxygraph.

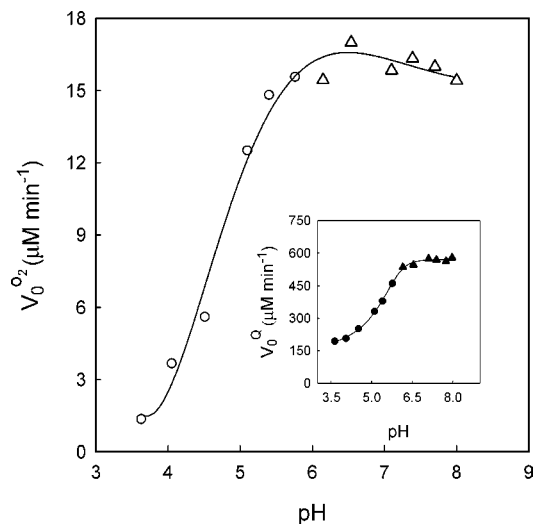


Figure 3. Catalase activity: pH-dependence of $V_0\text{O}_2$. The reactions were started by the addition of enzyme (63 nM) to reaction media containing H_2O_2 (9 mM) in 45 mM buffer (○) sodium phosphate, (△) sodium acetate. Inset: Diphenolase activity, pH-dependence of the initial rate of diphenol oxidation ($\lambda = 400$ nm). The reactions were started by the addition of enzyme (8.5 nM) to reaction media containing TBC (2 mM) in 45 mM sodium phosphate (●) or sodium acetate (▲).

participate in diphenolase activity also take part as intermediates in the catalase activity of tyrosinase (35).

Effect of pH. The pH profile for the catalase-like reaction of tyrosinase is shown in Figure 3. The rate of O_2 production increased at higher pH, indicating that acid media are unfavorable for the catalase cycle. The large pH dependence of the catalase activity of tyrosinase and the enzyme's saturation kinetics with H_2O_2 are analogous to peroxidase (20) but are different from catalase, whose activity is essentially pH independent in the pH range 4.7–10.5 (40). The activity curve

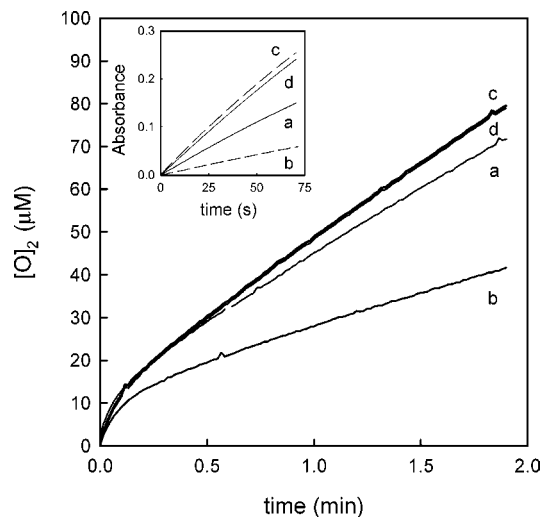


Figure 4. Effect of pH on the inhibition of catalase and diphenolase activity by chloride. (a) Catalase activity of tyrosinase at pH = 5 in 45 mM sodium acetate at 25 °C in the absence of chloride, $[H_2O_2]_0 = 9$ mM and $[E]_0 = 0.1$ μ M. (b) As (a) but with $[Cl^-]_0 = 10$ mM. (c) Catalase activity at pH = 7.0 in 45 mM sodium phosphate buffer at 25 °C in the absence of chloride. (d) As (c) but with $[Cl^-]_0 = 10$ mM. Inset: (a–d) As before but measuring diphenolase activity, $[TBC]_0 = 2$ mM and $[E]_0 = 4.4$ nM.

($V_0^{O_2}$ vs pH) in **Figure 3** is analogous to that for the catechol-oxidase activity of tyrosinase (**Figure 3**, inset), in which the participation of active site histidine residues in catalysis has been recognized (41). Therefore, the pH effect tends to indicate that the same active site residues are involved in the oxidation of *o*-diphenol (diphenolase activity) and the liberation of O_2 (catalase activity). Additionally, the similarity of the curves (**Figure 3**, inset) suggests the presence of the same critical pK in both types of activity, as is discussed later.

Action of Inhibitors. (a) *Inhibition by Chloride.* Halides are known to bind to the oxidized and reduced forms of tyrosinase (E_m and E_d) (42) inhibiting diphenolase activity. Also, in a recent stopped-flow fluorescence study of inhibitor binding to tyrosinase from *Streptomyces antibioticus* (43), it was shown that the inhibitor, fluoride ion, bound to the protonated enzyme ($E + H^+ \rightleftharpoons EH + F^- \rightleftharpoons EHF$), in the equatorial plane of the active site coppers. In the present study, we have examined the effects of chloride ion on tyrosinase's catalase and diphenolase activity (**Figure 4** and **Figure 4**, inset, respectively). Halide only binds to the acidic form of the enzyme, resulting in stronger inhibition with decreasing pH (43). **Figure 4** shows catalase activity in the absence of chloride at pH = 5.0 (curve a) and its presence (curve b). Similar behavior is also observed during diphenolase catalysis (**Figure 4**, inset, curves a and b). At pH = 7.0, neither reaction is affected by chloride (**Figure 4**, curves c and d, and **Figure 4**, inset, curves c and d). The explanation of inhibition is discussed later.

(b) *Inhibition by Troponone and Salicylhydroxamic Acid.* The slow inhibition of different tyrosinases by troponone has been widely described (44–46). It has been proposed that the inhibitor binds to E_{ox} as it accumulates during turnover (35). The affinity of E_{ox} for troponone is very high with $K_1^* = 1.4$ μ M (46). The effect of troponone on the catalase activity of tyrosinase was assayed. **Figure 5** shows that the addition of 2 μ M troponone had no effect on catalase activity, but the same concentration clearly produced time dependence inhibition of diphenolase activity (**Figure 5**, inset, curve c). This result shows that troponone did not affect the reaction of tyrosinase with H_2O_2 . As will be discussed later, during diphenolase activity practically

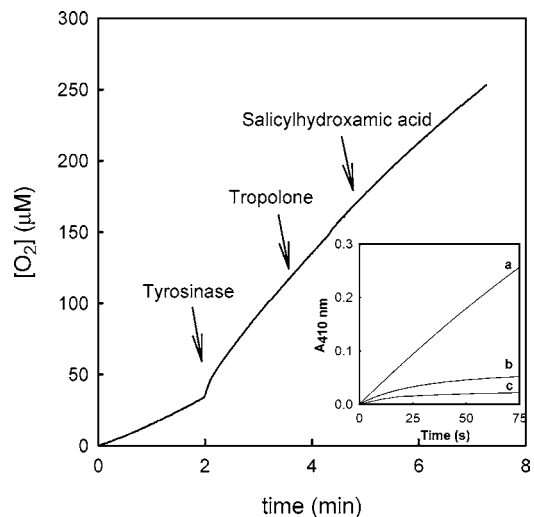


Figure 5. Inhibition of catalase and diphenolase activity by troponone and salicylhydroxamic acid. The reaction medium contained 45 mM sodium phosphate, pH = 6.5, $[H_2O_2]_0 = 9$ mM; tyrosinase (0.1 μ M), troponone (2 μ M), and salicylhydroxamic acid (2 μ M) were added at the times indicated. Inset: (a) TBC (2 mM) and tyrosinase (4.4 nM) in 1 mL of reaction medium. (b) As (a) but with troponone (2 μ M). (c) As (a) but with salicylhydroxamic acid (2 μ M).

all of the enzyme will be present as E_{ox} . However, it may be that during catalase activity the rate-limiting step leads to the accumulation under steady-state conditions of another enzymatic form with lower affinity for troponone. Furthermore, troponone binds to the active site coppers diaxially, whereas H_2O_2 binds equatorially and thus the two do not compete. A similar effect is seen with salicylhydroxamic acid, which is a potent inhibitor of tyrosinase (47, 48): a concentration of 2 μ M had no effect on catalase activity (**Figure 5**) but strongly inhibited diphenolase activity (**Figure 5**, inset, curve c). When diphenolase activity was measured as the consumption of O_2 , rather than product formation, inhibition was equally evident (results not shown).

Suicide Inactivation of Tyrosinase by H_2O_2 . The inactivation of tyrosinase by H_2O_2 was described some time ago (4, 6, 49), but changes of enzyme activity with time have not previously been followed using catalase activity. In the present work, the suicide inactivation of tyrosinase was observed by measuring catalase activity under both aerobic (**Figure 6**, curves a and b) and anaerobic conditions (**Figure 6**, curve c). The results indicated that inactivation was much more rapid when the incubation was performed anaerobically as compared to aerobically. The presence of O_2 reduces catalase activity, and thus the enzyme's turnover rate is lower resulting in protection from suicide inactivation.

Proposed Mechanism of Catalase Activity. From our previous work on the monophenolase and diphenolase activity of tyrosinase and the data presented in this study, we have proposed a kinetic and structural mechanism for the catalase activity of the enzyme (**Scheme 1**) (note the assignment of numbers to the rate constants has been done in such a way as to be consistent with the tyrosinase mechanism with monophenols and diphenols (35, 41, 50).) The catalytic cycle starts with the union of a molecule of H_2O_2 to form E_m (step 1). As was previously suggested in the diphenolase mechanism (35, 41), E_m contains a base, probably histidine, that at pH = 7.0 is deprotonated; this facilitates the interaction by forming a hydrogen bond to H_2O_2 and increases the possibility of a nucleophilic attack on the active site copper (Cu^{2+}) by

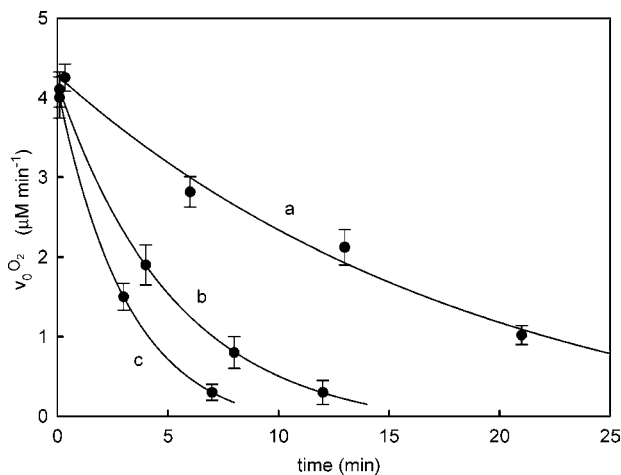
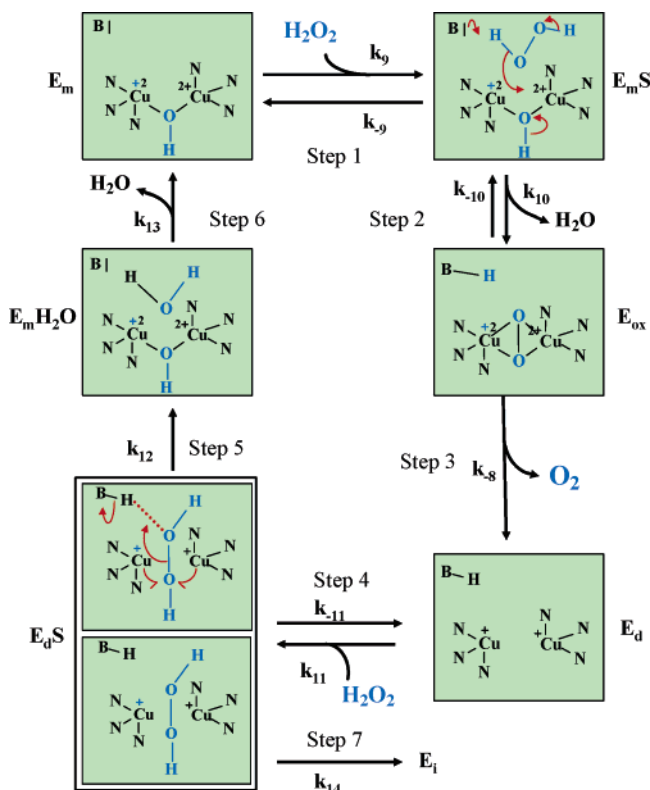


Figure 6. Suicide inactivation of the catalase activity of tyrosinase. The experimental conditions were as follows: incubation, 45 mM sodium phosphate buffer pH = 7.0, tyrosinase (0.6 μM). Aerobic conditions: (a) 5 mM H_2O_2 , (b) 30 mM H_2O_2 . Anaerobic conditions: (c) 30 mM H_2O_2 with continuous N_2 bubbling. At the times indicated, 100 μL aliquots were taken and then assayed for catalase activity (5 mM H_2O_2).

Scheme 1. Structural Mechanism Proposed To Explain the Tyrosinase Catalase Cycle^a

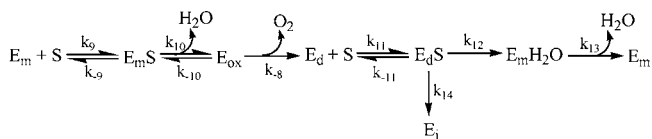


^a E_m , met-tyrosinase; E_{ox} , oxy-tyrosinase; E_d , deoxy-tyrosinase; B, acid-base catalyst; S, H_2O_2 ; $E_m\text{S}$, complex between E_m and S; $E_d\text{S}$, complex between E_d and S; E_i , inactive enzyme.

oxygen (step 2), and the subsequent loss of the other proton from the peroxide completes the union to the coppers to give E_{ox} .

In HRP-C, the distal histidine (His42) is also thought to be involved in catalase activity (21) from studies on the pH effect (20), acting as an acid/base catalyst. Studies using site-directed mutants of this residue (His42Glu) and also the reactive site arginine (Arg38Lys) showed that they are very important for HRP-C's catalase activity: $V_0\text{O}_2$ falls from 14.8 $\mu\text{M min}^{-1}$ for

Scheme 2



HRP-C* (recombinant wild-type) to 2.2 and 2.9 $\mu\text{M min}^{-1}$ for the respective mutants (21). In contrast, mutation of a residue of importance for phenolic substrate binding (Phe179Ser) or a surface residue (Ala140Gly), which has higher activity with ABTS than the wild-type, had little or no effect on catalase activity. Studies of the effect of pH on the catalase and diphenolase activities of tyrosinase (Figure 2) support this hypothesis. O_2 release is favored under anaerobic conditions (step 3) generating E_d . In this enzyme species, the base is protonated and does not aid the deprotonation of H_2O_2 , which would imply that the binding rate constant (k_{11}) (step 4) will be lower than that for the union with E_m (k_9) (step 1). The formation of a hydrogen bond between the protonated base and one of the peroxide oxygen atoms leads to the polarization of the O—O bond, facilitating the concerted oxidation of the two copper centers (step 5), and the subsequent liberation of a water molecule and formation of E_m . The pH dependence of catalase activity (Figure 3) supports the existence of a critical pK of the enzyme and at the same time explains why activity is reduced at lower pH; as is seen for diphenolase activity, the protonated enzyme is inactive. The mechanism predicts the stoichiometry: $2\text{H}_2\text{O}_2 \rightarrow \text{O}_2 + 2\text{H}_2\text{O}$. This was confirmed experimentally, working at low H_2O_2 and high enzyme concentrations, giving $2\text{H}_2\text{O}_2:1\text{O}_2$.

Over longer times in assays of catalase activity, a loss of activity is observed (Figure 6, curves a and b under aerobic, and c under anaerobic conditions). At a mechanistic level (Scheme 1), the inactivation of tyrosinase may be explained by step 7. If oxidation of the two coppers is not concerted, an inactive enzyme species may form, possibly via a radical mechanism accompanied by formation of hydroxyl radicals ($\text{HO}\bullet$) that attack histidines in the active site and could cause the coppers to be lost as has been described in the suicide inactivation of tyrosinase during turnover with monophenols and diphenols (52). Note that the suicide inactivation of the monophenolase and diphenolase activity of mushroom tyrosinase has previously been kinetically analyzed by us (53).

The proposed mechanism (Scheme 1) also explains the behavior of the different inhibitors tested. Chloride binds equatorially to the active site coppers in the enzyme at acid pH ($E_m\text{H}$) reducing the enzyme available for both activities (catalase and diphenolase) (Figure 4). Thus, at pH = 7.0, when the enzyme is deprotonated, chloride does not inhibit either catalase (Figure 4) or diphenolase (Figure 4, inset) activity. However, at pH = 5.0, when the enzyme is mainly present as $E_m\text{H}$, chloride binds to this form and inhibits both activities to the same extent (Figure 4 and Figure 4, inset). In the case of tropolone and salicylhydroxamic acid, shown in Figure 5 and Figure 5, inset, for catalase and diphenolase activities, respectively, the differences in behavior observed can be explained by the kinetics on the mechanism as discussed in the following section.

Kinetic Analysis. The mechanism shown in Scheme 1 can be redrawn as shown in Scheme 2 where S is H_2O_2 , E_m , E_{ox} , and E_d are the enzymatic species involved in turnover, and E_i is inactive tyrosinase. At short reaction times, the concentration of E_i is negligible (given that k_{14} is small) and the system reaches a pseudo-steady state. The analytical expression for the initial

velocity of O₂ formation is:

$$V_0^{O_2} = \frac{\alpha[S]_0[E]_0}{\beta + [S]_0} \quad (2)$$

where

$$\alpha = (k_{-8}k_{+9}k_{+10}k_{+11}k_{+12}k_{+13}) / (k_{+9}k_{-10}k_{+11}k_{+12}k_{+13} + k_{+9}k_{-8}k_{+11}k_{+12}k_{+13} + k_{+9}k_{+10}k_{+11}k_{+12}k_{+13} + k_{+9}k_{+10}k_{-8}k_{+11}k_{+13} + k_{+9}k_{+10}k_{-8}k_{+11}k_{+12}) \quad (3)$$

and

$$\beta = (k_{-9}k_{-10}k_{+11}k_{+12}k_{+13} + k_{-9}k_{-8}k_{+11}k_{+12}k_{+13} + k_{+10}k_{-8}k_{+11}k_{+12}k_{+13} + k_{+9}k_{+10}k_{-8}k_{-11}k_{+13} + k_{+9}k_{+10}k_{-8}k_{+12}k_{+13}) / (k_{+9}k_{-10}k_{+11}k_{+12}k_{+13} + k_{+9}k_{-8}k_{+11}k_{+12}k_{+13} + k_{+9}k_{+10}k_{-8}k_{+11}k_{+13} + k_{+9}k_{+10}k_{-8}k_{+11}k_{+12}) \quad (4)$$

The binding of S to E_m controlled by k₉ (helped by the base, see **Scheme 1**) is faster than its binding to E_d (governed by k₁₁), that is, k₉ > k₁₁. In an exhaustive study of mushroom *oxy*-tyrosinase Mason et al. (6) determined the binding and dissociation rate constants of H₂O₂ and E_m giving (**Scheme 1**) k₉ = 675 M⁻¹ s⁻¹ and k₋₉ = 8.0 × 10⁻⁴ s⁻¹; thus, E_m has a high affinity for H₂O₂ and K_S = k₋₉/k₉ = 1.1 × 10⁻⁶ M. It is unlikely, therefore, that E_m is responsible for the value of K_m^{H₂O₂} (29.7 ± 4.2) mM and much more probable that it is due to the form E_d. With respect to the relative values of k₋₁₁ and k₋₉, it is clear that k₋₁₁ > k₋₉ because there is no nucleophilic attack in the binding of H₂O₂ to E_d and dissociation is favorable in this case.

The rate of O₂ release controlled by k₋₈ is (1.07 ± 0.2) × 10³ s⁻¹ (35), and, therefore, given that k_{cat} is (16.4 ± 1.1) s⁻¹, it follows that k₋₈ > k₁₂. From this, if the release of H₂O controlled by k₁₃ is fast, then from eq 2, the expression of V₀^{O₂} is given in eq 5.

$$V_0^{O_2} = \frac{k_{12}[S]_0[E]_0}{\frac{k_{12} + k_{-11}}{k_{11}} + [S]_0} \quad (5)$$

This gives K_m^{H₂O₂} ≈ k₋₁₁ + k₁₂/k₁₁ and using a rapid equilibrium approximation, K_m^{H₂O₂} ≈ k₋₁₁/k₁₁. This relationship can result in low affinity (29.7 ± 4.2) mM and control the catalase activity of tyrosinase. Note that from the instability of E_{ox}, weak catalase activity (low k₁₂) has previously been proposed with an optimum at pH = 6.5 (6), which is in agreement with **Figure 3**.

In the mechanism of tyrosinase with *o*-diphenols (35), the binding of substrate to E_m is faster than to E_{ox}, meaning that the steady-state concentration of E_{ox} is high and it undergoes slow inhibition by tropolone and salicylhydroxamic acid (**Figure 5** and **Figure 5**, inset). However, in the case of the mechanism of tyrosinase with H₂O₂, substrate binding is faster with E_m than with E_d, and, because the rate constant of O₂ release from E_{ox} (k₋₈) is very high, in the steady state the concentration of E_{ox} is negligible. Thus, tropolone and salicylhydroxamic acid cannot inhibit E_{ox}, and it is E_d that most accumulates in the medium. The Cu–Cu distance in the active site has been calculated for sweet potato catechol oxidase, in the reduced, E_d (Cu¹⁺Cu¹⁺), and the oxidized forms, E_m (Cu²⁺Cu²⁺), yielding 4.4 versus 2.9 Å, respectively (54). Possibly due to this difference, E_d has lower affinity for *o*-diphenol analogues, such as tropolone and

salicylhydroxamic acid, and at the concentrations assayed (**Figure 5**) they do not inhibit the enzyme. On the other hand, because these inhibitors bind diaxially E_d can still bind H₂O₂ in the equatorial plane of the coppers.

Similarities to and Differences from Other Mechanisms.

The proposed mechanism presents similarities to that previously described for the catalase activity of hemocyanines (13–15). It should be noted that, in tyrosinase, the presence of a base (i.e., histidine) has been postulated that forms a hydrogen bond to the H₂O₂ (see **Scheme 1**).

With respect to the proposed mechanism of CAO (8), the fundamental difference is that it has been suggested that two molecules of H₂O₂ bind to E_m before O₂ is released. This would yield a quadratic analytical rate equation for V₀^{O₂}; such dependence is not supported by the experimental data for tyrosinase. Furthermore, the binding and activation of the second H₂O₂ molecule is facilitated by the orientation of the Glu236 residue whose carboxy group permits monodentate binding of this peroxide molecule to Cu B. Thus, the catalase activity of a 39 kDa isoenzyme of *Ipomea batatas* (sweet potato) catechol oxidase could be explained by the substitution of Thr243 (40 kDa isoenzyme) by Ile241 (39 kDa isoenzyme), affecting the orientation of the Glu238/236 residue. It is noteworthy that, working with tyrosinase from *Streptomyces glaucescens* (55), the substitution of Asp208, a residue in the region of Cu B, for Glu resulted in the stabilization of E_{ox} in the equilibrium E_{ox} ⇌ E_m + O₂²⁻, revealing the influence of the structure for the stability of the intermediates. Studies on the catalase activity of Cu²⁺ complexes have demonstrated that free coordination sites must be available to enable the formation of the ternary Cu²⁺-peroxo ligand complexes required for catalysis (56). Additional evidence supporting our mechanism comes from the reaction of Cu²⁺ complexes with H₂O₂: in all of the cases described, the first molecule of H₂O₂ must be deprotonated to nucleophilically attack the Cu²⁺: H₂O₂ ⇌ HOO⁻ + H⁺ (56). This nucleophilic attack must be the limiting step because the concerted release of the proton is required to increase oxygen's nucleophilicity. In our mechanism, this same step, controlled by k₉ (**Scheme 1**), is not limiting because base B (**Scheme 1**) favors the deprotonation of H₂O₂ and the nucleophilic attack on the copper. The other proton transfers to the bridge between the two copper centers and water is released. The liberation of O₂ (Step 3) is rapid with a previously determined constant, k₋₈ = (1.07 ± 0.2) × 10³ s⁻¹ (35).

The binding of H₂O₂ to E_d (controlled by k₁₁) is not facilitated by the base because it is protonated and in consequence must be slow. Additionally, the transformation constants, k₁₂ (**Scheme 1**), must be smaller than k₋₈, given that in this step various concerted reactions must occur, such as polarization of the peroxide O–O bond, due to the formation of a hydrogen bond between the protonated base and an oxygen in the peroxide, followed by concerted oxidation of the two coppers.

Possible Physiological Implications. Tyrosine catalyzes the first steps of melanogenesis (1). However, other activities have been described because of its low substrate specificity: pseudocatalase (6), pseudoperoxidase (57–59), and ascorbate oxidase activity (60). In this study, the kinetics and mechanism of catalase activity have been examined in depth, and it is worth considering if a physiological function for this activity exists. Large amounts of H₂O₂ are produced in human tumor cells (61) and also in plants during the oxidation of catechin (62). An effect of H₂O₂ on the induction of tyrosinase biosynthesis has also been described (33). In the final steps of melanogenesis, the formation of H₂O₂ has been demonstrated (63), and, although

abundant tyrosinase and catalase is observed in melanomas, only low levels of catalase are detected in patients with vitiligo (64). Thus, the catalase activity of tyrosinase could possibly be important (a) to reduce H₂O₂ concentrations, (b) in anaerobic conditions, to hydroxylate monophenols and oxidize diphenols because H₂O₂ forms E_{ox}, (c) to reduce anaerobiosis by generating O₂ from H₂O₂, and (d) to produce *o*-quinones as a defense against pathogens.

In conclusion, the catalase activity of mushroom tyrosinase has been kinetically characterized. A kinetic and structural mechanism consistent with the experimental results has been proposed. The action of different types of inhibitors has been discussed, and the suicide inactivation of tyrosinase by H₂O₂ in the absence of reducing substrates has been described.

ABBREVIATIONS USED

ABTS, 2,2'-azino-bis-(3-ethylbenzthiazoline-6-sulfonic acid); CAO, catechol oxidase; HRP, horseradish peroxidase; H₂O₂, hydrogen peroxide; O₂^{•-}, superoxide radical anion; SOD, superoxide dismutase.

LITERATURE CITED

- Prota, G.; d'Ischia, M.; Napolitano, A. The chemistry of melanins and related metabolites. In *The Pigmentary System*; Nordlund, J. J., Boissy, R., Hearing, V., King, R., Ortonne, J. P., Eds.; University Press: Oxford, 1998.
- Vámos-Vigázó, L. Prevention of enzymatic browning in fruits and vegetables: a review of principles and practice. In *Enzymatic browning and its prevention*; Lee, C. Y., Whitaker, J. R., Eds.; American Chemical Society: Washington, DC, 1995.
- Whitaker, J. R.; Lee, C. Y. Recent advances in chemistry of enzymatic browning: An overview. In *Enzymatic browning and its prevention*; Lee, C. Y., Whitaker, J. R., Eds.; American Chemical Society: Washington, DC, 1995.
- Jolley, R. L.; Evans, L. H.; Mason, H. S. Reversible oxygenation of tyrosinase. *Biochem. Biophys. Res. Commun.* **1972**, *46*, 878–884.
- Makino, N.; Mason, H. S. Reactivity of oxytyrosinase towards substrates. *J. Biol. Chem.* **1973**, *248*, 5731–5735.
- Jolley, R. L.; Evans, L. H.; Makino, N.; Mason, H. S. Oxytyrosinase. *J. Biol. Chem.* **1974**, *249*, 335–345.
- Ros-Martinez, J. R.; Rodríguez-López, J. N.; Castellanos, R. V.; García Cánovas, F. Discrimination between two kinetic mechanisms for the monophenolase activity of tyrosinase. *Biochem. J.* **1993**, *294*, 621–623.
- Gerdemann, C.; Eicken, C.; Magrini, A.; Meyer, H. E.; Rompel, A.; Spener, F.; Krebs, B. Isozymes of *Ipomoea batatas* catechol oxidase differ in catalase-like activity. *Biochim. Biophys. Acta* **2001**, *1548*, 94–105.
- Solomon, E. I.; Sundaram, U. M.; Machonkin, T. E. Multicopper oxidases and oxygenases. *Chem. Rev.* **1996**, *96*, 2563–2605.
- Decker, H.; Rimke, T. Tarantula hemocyanin shows phenol-oxidase activity. *J. Biol. Chem.* **1998**, *273*, 25889–25892.
- Decker, H.; Tuzcek, F. Tyrosinase/catecholoxidase activity of hemocyanins: structural basis and molecular mechanism. *Trends Biochem. Sci.* **2000**, *25*, 392–397.
- Himmelwright, R. S.; Eickman, N. C.; Lubien, K. D.; Lerck, K.; Solomon, E. I. Chemical and spectroscopic comparison of the binuclear copper active site of mollusc and arthropod hemocyanins. *J. Am. Chem. Soc.* **1980**, *102*, 7339–7344.
- Ghiretti, F. The decomposition of hydrogen peroxide by hemocyanin and by its dissociation products. *Arch. Biochem. Biophys.* **1956**, *63*, 165–176.
- Felsenfeld, G.; Printz, M. P. J. Specific reaction of hydrogen peroxide with the active site of hemocyanin. The formation of methemocyanin. *J. Am. Chem. Soc.* **1959**, *81*, 6259–6264.
- Zlaterva, T.; Santagostini, L.; Bubacco, L.; Casella, L.; Salvato, B.; Beltrami, M. J. Isolation of the met-derivative intermediate in the catalase-like activity of deoxygenated *Octopus vulgaris* hemocyanin. *J. Inorg. Biochem.* **1998**, *72*, 211–215.
- Dunford, H. B. Other class I peroxidases: ascorbate peroxidase and bacterial catalase-peroxidase. *Heme peroxidases*; Wiley-VCH: New York, 1999; pp 270–280.
- Welinder, K. G. Superfamily of plant, fungal and bacterial peroxidases. *Curr. Opin. Struct. Biol.* **1992**, *2*, 388, 393.
- Hiner, A. N. P.; Rodríguez Lopez, J. N.; Arnao, M. B.; Raven, E. R.; García Cánovas, F. A kinetic study of the inactivation of ascorbate peroxidase by hydrogen peroxide. *Biochem. J.* **2000**, *348*, 321–328.
- Hiner, A. N. P.; Hernandez Ruiz, J.; Rodríguez López, J. N.; García Cánovas, F.; Brisset, N. C.; Smith, A. T.; Arnao, M. B.; Acosta, M. Reactions of the class II peroxidases, lignin peroxidase and *Arthromyces ramosus* peroxidase with hydrogen peroxide. Catalase-like activity, compound III formation, and enzyme inactivation. *J. Biol. Chem.* **2002**, *277*, 26879–26885.
- Hernandez-Ruiz, J.; Arnao, M. B.; Hiner, A. N. P.; García-Cánovas F.; Acosta, M. Catalase-like activity of horseradish peroxidase: relationship to enzyme inactivation by H₂O₂. *Biochem. J.* **2001**, *354*, 107–114.
- Hiner, A. N. P.; Hernandez-Ruiz, J.; Williams, G. A.; Arnao, M. A.; García-Cánovas, F.; Acosta, M. Catalase-like oxygen production by horseradish peroxidase must predominantly be an enzyme-catalyzed reaction. *Arch. Biochem. Biophys.* **2001**, *392*, 295–302.
- Hiner, A. N. P.; Hernandez-Ruiz, J.; Rodríguez-López, J. N.; Arnao, M. A.; Varón, R.; García-Cánovas, F.; Acostar, M. The inactivation of horseradich peroxidase isoenzyme A2 by hydrogen peroxide: an example of partial resistance due to the formation of a stable enzyme intermediate. *J. Biol. Inorg. Chem.* **2001**, *6*, 504–516.
- Hernandez-Ruiz, J.; Rodríguez-López, J. N.; García-Cánovas, F.; Acostar, M.; Arnao, M. A. Characterization of isoperoxidase-B2 inactivation in etiolated *Lupinus albus* hypocotyls. *Biochim. Biophys. Acta* **2000**, *1478*, 78–88.
- Sun, W.; Kadima, T. A.; Rickard, M. A.; Dunford, H. B. Catalase activity of chloroperoxidase and its interaction with peroxidase activity. *Biochem. Cell Biol.* **1994**, *72*, 321–331.
- Hochman, A.; Golberg I. Purification and characterization of a catalase-peroxidase and a typical catalase from the bacterium *Klebsiella pneumoniae*. *Biochim. Biophys. Acta* **1991**, *1077*, 299–307.
- Obinger, C.; Regelsberger, G.; Pircher, A.; Sevcik-Klöckler, A.; Strasser, G.; Peschek, G. A. Hydrogen peroxide removal in cyanobacteria. Characterization of a catalase-peroxidase from *Anacystis nidulans*. In *The Phototrophic Prokaryotes*; Peschek, et al., Eds.; Kluwer Academic: New York, 1999.
- Hiner, A. N.; Hernández-Ruiz, J.; Arnao, M.; García-Cánovas, F.; Acosta, M. A. Comparative study of the purity, enzyme activity, and inactivation by hydrogen peroxide of commercially available horseradish peroxidase isoenzymes A and C. *Bio-technol. Bioeng.* **1996**, *50*, 655–662.
- Rodríguez-López, J. N.; Hernández-Ruiz, J.; García-Cánovas, F.; Thorneley, R. N. F.; Acosta, M. A.; Arnao, M. B. The inactivation and catalytic pathways of horseradish peroxidase with *m*-chlorophenoxybenzoic acid: a spectrophotometric and transient kinetic study. *J. Biol. Chem.* **1997**, *272*, 5469–5476.
- Jackson, P.; Pulo, S.; Pinto, R. E. B2, the major soluble peroxidase of lupins, in vegetative development and the plant response to pathogenic agents. In *Plant Peroxidases: Biochemistry and Physiology*; Obinger, C., Burner, U., Ebermann, R., Perner, C., Greppin, H., Eds.; University of Geneva: Switzerland, 1996; ppp 247–253.
- Acosta, M.; Casas, J. L.; Arnao, M. B.; Sabater, F. 1-Aminocyclopropane-1-carboxylic acid as a substrate of peroxidase: conditions for oxygen consumption, hydroperoxide generation and ethylene production. *Biochim. Biophys. Acta* **1991**, *1077*, 273–280.

- (31) Cano, A.; Artés, F.; Arnao, M. B.; Sánchez-Bravo, J.; Acosta, M. Influences of peroxides, ascorbate and glutathione on germination and growth in *Lupinus albus* L. *Biol. Plant.* **1997**, *39*, 257–266.
- (32) Noctor, G.; Foyer, C. H. Ascorbate and glutathione: keeping active oxygen under control. *Annu. Rev. Plant. Physiol. Mol. Biol.* **1998**, *177*, 1103–1114.
- (33) Karg, E.; Dalh, G.; Wittbjer, A.; Rosengren, E.; Rorsman, H. Hydrogen peroxide as an inducer of elevated tyrosinase level in melanoma cells. *J. Invest. Dermatol.* **1993**, *100*, 209S–213S.
- (34) Duckworth, H. W.; Coleman, J. E. Physicochemical and kinetic properties of mushroom tyrosinase. *J. Biol. Chem.* **1970**, *245*, 1613–1625.
- (35) Rodríguez Lopez, J. N.; Fenoll, L. G.; García-Ruiz, J.; Varón, R.; Tudela, J.; Thornely, R. N.; García Cánovas, F. Stopped-flow and steady-state study of the diphenolase activity of mushroom tyrosinase. *Biochemistry* **2000**, *39*, 10497–10506.
- (36) Bradford, M. M. A rapid and sensitive method for the quantification of microgram quantities of proteins utilising the principle of protein-dye binding. *Anal. Biochem.* **1976**, *72*, 248–256.
- (37) Waite, J. H. Calculating extinction coefficients for enzymatically produced o-quinones. *Anal. Biochem.* **1976**, *75*, 211–218.
- (38) Rodríguez-López, J. N.; Ros Martínez, J. R.; Varón, R.; García Cánovas, F. Calibration of a Clark-type electrode by tyrosinase-catalyzed oxidation of 4-*tert*-butylcatechol. *Anal. Biochem.* **1992**, *202*, 1–5.
- (39) Jandel Scientific. *Sigma Plot 2.01 for Windows*; Jandel Scientific: Core Madera, 1994.
- (40) Dunford, H. B. *Catalases. Heme peroxidases*; Wiley-VCH: New York, 1999; pp 435–453.
- (41) Fenoll, L. G.; Rodríguez López, J. N.; García Sevilla, F.; García Ruiz, P. A.; Varón, R.; García Cánovas, F.; Tudela, J. Analysis and interpretation of the action mechanism of mushroom tyrosinase on monophenols and diphenols generating highly instable o-quinones. *Biochim. Biophys. Acta* **2001**, *1548*, 1–22.
- (42) Tepper, A. W. J. W.; Bubbacco, L.; Canters, G. W. Structural basis and mechanism of the inhibition of the type-3 copper protein tyrosinase from *Streptomyces antibioticus* by halide ions. *J. Biol. Chem.* **2002**, *277*, 30436–30444.
- (43) Tepper, A. W. J. W.; Bubbacco, L.; Canters, G. W. Stopped-flow fluorescence studies of inhibitor binding to tyrosinase from *Streptomyces antibioticus*. *J. Biol. Chem.* **2004**, *279*, 13425–13434.
- (44) Kahn, V.; Andrawis, A. Inhibition of mushroom tyrosinase by tropolone. *Phytochemistry* **1985**, *24*, 905–908.
- (45) Valero, E.; García-Moreno, M.; Varón, R.; García-Carmona, F. Time-dependent inhibition of grape polyphenol oxidase by tropolone. *J. Agric. Food Chem.* **1991**, *39*, 1043–1046.
- (46) Espín, J. C.; Wichers, H. J. Slow-binding inhibition of mushroom (*Agaricus bisporus*) tyrosinase isoforms by tropolone. *J. Agric. Food Chem.* **1999**, *47*, 2638–2644.
- (47) Rich, P. R.; Wiegand, N. K.; Blum, H.; Moore, A. L.; Bonner, W. D., Jr. Studies on the mechanism of inhibition of redox enzymes by substituted hydroxamic acids. *Biochim. Biophys. Acta* **1978**, *525*, 325–337.
- (48) Kahn, V. Effect of acetohydroxamic acid (AHA) and salicylhydroxamic acid (Sham) on the oxidation of o-dihydroxy and trihydroxyphenols by mushroom tyrosinase. *J. Food Biochem.* **1999**, *23*, 409–433.
- (49) Kahn, V. Multiple effects of hydrogen peroxide on the activity of avocado polyphenol oxidase. *Phytochemistry* **1983**, *22*, 2155–2159.
- (50) Sánchez-Ferrer, A.; Rodríguez-Lopez, J. N.; García-Cánovas, F.; García Carmona, F. Tyrosinase: A comprehensive review of its mechanism. *Biochim. Biophys. Acta* **1995**, *1247*, 1–11.
- (51) Veitch, N. C.; Gao, Y.; Smith, A. T.; White, C. G. Identification of a critical phenylalanine residue in horseradish peroxidase, Phe179, by site-directed mutagenesis and 1H-NMR: implications for complex formation with aromatic donor molecules. *Biochemistry* **1997**, *36*, 14751–61.
- (52) Dietler, C.; Lerch, K. In *Oxidases and Related Redox Systems*; King, T. E., Ed.; Pergamon Press: Oxford, 1982; pp 305–317.
- (53) Cánovas, F. G.; Tudela, J.; Madrid, C. M.; Varón, R.; Carmona, F. G.; Lozano, J. A. Kinetic study on the suicide inactivation of tyrosinase induced by catechol. *Biochim. Biophys. Acta* **1987**, *912*, 417–423.
- (54) Klabunde, T.; Eicken, C.; Sacchetti, J. C.; Krebs, B. Crystal structure of a plant catechol oxidase containing a dicopper center. *Nat. Struct. Biol.* **1998**, *12*, 1084–90.
- (55) Jackman, M. P.; Huber, M.; Hajnal, A.; Lerch, K. Stabilization of the oxy form of tyrosinase by a single conservative amino acid substitution. *Biochem. J.* **1992**, *282*, 915–8.
- (56) Sigel, H. Catalase and peroxidase activity of Cu²⁺ complexes. *Angew. Chem., Int. Ed. Engl.* **1969**, *8*, 167–177.
- (57) Strothkamp, K. G.; Mason, H. S. Pseudoperoxidase activity of mushroom tyrosinase. *Biochem. Biophys. Res. Commun.* **1974**, *21*, 827–832.
- (58) Jimenez, M.; García-Carmona, F. Hydrogen peroxide-dependent 4-*tert*-butylphenol hydroxylation by tyrosinase: a new catalytic activity. *Biochim. Biophys. Acta* **1996**, *1297*, 33–9.
- (59) Jimenez, M.; García-Carmona, F. Hydroxylating activity of tyrosinase and its dependence on hydrogen peroxide. *Arch. Biochem. Biophys.* **2000**, *373*, 255–60.
- (60) Ros, J. R.; Rodríguez-Lopez, J. N.; Varon-Catellanos, R.; García-Cánovas, F. Mushroom tyrosinase has an ascorbate oxidase activity. *Biochem. Mol. Biol. Int.* **1995**, *36*, 301–309.
- (61) Szatrowski, T. P.; Nathan, C. F.; Production of large amounts of hydrogen peroxide by human tumor cell. *Cancer Res.* **1991**, *51*, 794–798.
- (62) Jiang, Y.; Riles, P. W. Generation of H₂O₂ during enzymic oxidation of catechin. *Phytochemistry* **1993**, *33*, 29–34.
- (63) Nappi, A. J.; Vass, E. Hydrogen peroxide generation associated with the oxidations of the eumelanin precursors 5,6-dihydroxyindole and 5,6-dihydroxyindole-2-carboxylic acid. *Melanoma Res.* **1996**, *6*, 541–549.
- (64) Schallreuter, K. U.; Wood, J. M.; Berger, J. Low catalase levels in the epidermis of patients with vitiligo. *J. Invest. Dermatol.* **1991**, *97*, 1081–1085.

Received for review October 5, 2004. Revised manuscript received February 8, 2005. Accepted March 4, 2005. This work was supported in part by CICYT, Spain, project AGL 2002-01255 ALI and the Fundación Séneca/Consejería de Agricultura, Agua y Medio Ambiente, Murcia, project AGR/10/FS/02 (F.G.-C.), and by the Fundación Séneca/Consejería de Educación y Cultura, Murcia, project PI-79/00810/FS/01 (J.T.). A.N.P.H. has a contract with ArtBiochem S.L., Murcia. L.G.F. has a postdoctoral fellowship from the University of Murcia. F.G.-M. has a predoctoral fellowship from MEC, Spain.